Insertion Reactions of CO and CO_2 with Ruthenium Benzyl, Arylamido, and Aryloxide Complexes: A Comparison of the Reactivity of Ruthenium–Carbon, Ruthenium–Nitrogen, and Ruthenium–Oxygen Bonds

John F. Hartwig, Robert G. Bergman,* and Richard A. Andersen*

Contribution from the Department of Chemistry, University of California, Berkeley, California 94720. *Received September 21, 1990*

Abstract: An investigation of the mechanism and selectivies of CO and CO_2 insertion reactions into four-membered metallacycles containing Ru–O, Ru–N, benzylic Ru–C, and aryl Ru–C bonds was conducted. The reaction of carbon monoxide with $(PMe_3)_4Ru(\eta^2\text{-}CH_2C_6H_4)$ (**1**), $(PMe_3)_4Ru(\eta^2\text{-}OC_6H_3Me)$ (**2**), and $(PMe_3)_4Ru(\eta^2\text{-}NHC_6H_4)$ (**3**) provides products resulting from insertion of CO into the metal–aryl bond and replacement of one PMe_3 ligand with CO. Reaction of CO_2 with $(PMe_3)_4Ru(\eta^2\text{-}CH_2C_6H_4)$ (**1**) or $(PMe_3)_4Ru(\eta^2\text{-}OC_6H_3Me)$ (**2**) in arene solvent also occurs at the metal–aryl bond, while reaction of CO_2 with $(PMe_3)_4Ru(\eta^2\text{-}CH_2C_6H_4)$ (**1**) in pentane results in insertion into the ruthenium–aryl bond and dissociation of PMe_3 to give $(PMe_3)_3Ru(\eta^4\text{-}CH_2C_6H_4CO_2)$. In contrast to these reactions with the metal–aryl bond, reaction of CO_2 with $(PMe_3)_4Ru(\eta^2\text{-}NHC_6H_4)$ (**3**) results in a formal insertion into the metal–nitrogen bond. Low-temperature NMR experiments demonstrate that reaction of **3** with CO_2 occurs by direct attack of the CO_2 at the nitrogen atom of the metallacycle, followed by rearrangement to the final product (**11**). Thermolysis of insertion product **11** at 120 °C for 2 h led to formation of the carboxamide complex $(PMe_3)_4Ru(\eta^2\text{-}OC(O)NPh)$ (**15**), independently prepared during the course of a separate study; no rearrangement to the anthranilic acid dianion complex $(PMe_3)_4Ru(\eta^2\text{-}NHC_6H_4C(O)O)$ (**13**), the formal insertion product of CO_2 into the ruthenium–aryl bond, was observed. The anthranilate complex **13** was independently synthesized to determine if it rearranges to the direct insertion product **11** or is stable to the thermolysis conditions leading to the rearrangement of **11**. Thermolysis did not lead to the product of insertion into the metal nitrogen bond or to the carboxamide complex formed from **11** at these temperatures. Instead, it underwent a reversible proton transfer and ring contraction to form the carbon and oxygen bound anthranilate complex $(PMe_3)_4Ru(\eta^2\text{-}OC(O)C_6H_3(NH_2))$ (**17**).

Introduction

Transition metal–carbon, –oxygen, and –nitrogen bonds are involved in many homogeneous and heterogeneous catalytic processes.[1] Although late transition metal–carbon bonds have been carefully studied for many years, examples of late transition metal–oxygen and –nitrogen linkages have only recently been actively investigated.[2] It has been thought that late transition metal alkoxide and amide complexes would be unstable due to the poor match of a soft metal system with a traditionally hard ligand.[3] Yet, several monomeric alkoxide and amide complexes have now been isolated in 16-electron square-planar complexes,[4] as well as 18-electron octahedral and pseudooctahedral geometries.[5]

Reactions such as reductive elimination and migratory insertion, which are well understood with metal–carbon bonds, have been observed with only a few systems containing late transition metal–oxygen and –nitrogen bonds.[4b-h,6,7] Insertions of carbon monoxide, carbon dioxide, and alkenes into transition metal alkyl bonds have attracted the most attention, and recently the insertion of these substituents into late transition metal alkoxide and amide linkages has been observed. Examples of insertion reactions involving platinum alkoxide and amide linkages exist,[6,7] as do insertions into both 16-electron and 18-electron iridium and rhodium alkoxide bonds.[4d-f,5a] Some kinetic[5a,6f] and labeling[6g] data have been obtained for these reactions, and complexes which may model reaction intermediates have been isolated or observed.[4f,7] Nevertheless, the little information that is available on these reactions has not led to a clear mechanistic picture. Some authors

Scheme I

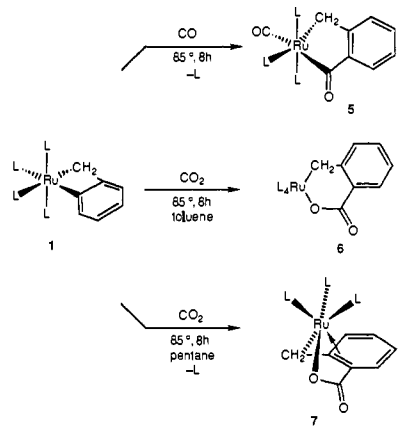

(1) Masters, C *Homogeneous Transition-Metal Catalysis*; Chapman and Hall: New York, 1981.
(2) Bryndza, H. E.; Tam, W. *Chem. Rev.* **1988**, *88*, 1163.
(3) (a) Pearson, R. G. *J. Am. Chem. Soc.* **1963**, *85*, 3533. (b) Pearson, R. G. *J. Chem. Educ.* **1968**, *45*, 643. (c) Hartley, F. R. *The Chemistry of Platinum and Palladium*; Wiley: New York, 1976; p 169. (d) Lappert, M. F.; Power, P. P.; Sanger, A. R.; Srivastava, R. C. *Metal and Metalloid Amides*; Ellis Harwood; Chinchester, 1980.
(4) (a) Bryndza, H. E.; Fong, L. K.; Paciello, R. A.; Tam, W.; Bercaw, J. E. *J. Am. Chem. Soc.* **1987**, *109*, 1444. (b) Kim, Y-J.; Osakada, K.; Sugita, K.; Yamamoto, T.; Yamamoto, A. *Organimetallics* **1988**, *7*, 2182. (c) Komiya, S.; Akai, Y.; Tanaka, K.; Yamamoto, T.; Yamamoto, A. *Organometallics* **1985**, *4*, 1130. (d) Yoshida, T.; Okano, T.; Ueda, Y.; Otsuka, S. *J. Am. Chem. Soc.* **1981**, *103*, 3411. (e) Rees, W. M.; Churchill, M. R.; Fettinger, J. C.; Atwood, J. D. *Organometallics*, **1985**, *4*, 2179. (f) Rees, W. M.; Atwood, J. D. *Organometallics* **1985**, *4*, 402. (g) Cowan, R. L.; Trogler, W. C. *J. Am. Chem. Soc.* **1989**, *111*, 4750. (h) Bugro, C. D.; Pasquali, M.; Leoni, P.; Subatino, P.; Braga, D. *Inorg. Chem.* **1989**, *28*, 1390.
(5) (a) Newman, L. J.; Bergman, R. G. *J. Am. Chem. Soc.* **1985**, *107*, 5314. (b) Milstein, D.; Calabrese, J. C.; Williams, I. D. *J. Am. Chem. Soc.* **1986**, *108*, 6387. (c) Darensbourg, D. J.; Sanchez, K. M.; Rheingold, A. L. *J. Am. Chem. Soc.* **1987**, *109*, 290. (d) Hartwig, J. F.; Andersen, R. A.; Bergman, R. G. *J. Am. Chem. Soc.* **1989**, *111*, 2717. (e) Milstein, D. *J. Am. Chem. Soc.* **1986**, *108*, 3525. (f) Dewey, M. A.; Arif, A. M.; Gladysz, J. A. *J. Chem. Soc., Chem. Commun.* **1991**, 712 and references cited therein.
(6) (a) Bennett, M. A.; Yoshida, T. *J. Am. Chem. Soc.* **1978**, *100*, 1750. (b) Arnold, D. P.; Bennett, M. A.; Crisp, G. T.; Jeffery, J. C. *Adv. Chem. Ser.* **1982**, *No. 196*, 195. (c) Michelin, R. A.; Napoli, M.; Ros, R. *J. Organomet. Chem.* **1979**, *175*, 239. (d) Bennett, M. A. *J. Organomet. Chem.* **1986**, *300*, 7. (e) Bennett, M. A.; Rokicki, A. *J. Organomet. Chem.* **1979**, *175*, 239. (f) Bryndza, H. E. *Organometallics* **1985**, *4*, 1686. (g) Bryndza, H. E.; Calabrese, J. C.; Reford, S. S. *Organometallics* **1984**, *3*, 1603. (h) Bryndza, H. E.; Kretchmer, S.; Tulip, T. H. *J. Chem. Soc., Chemm. Commun.* **1985**, 977. (i) Bryndza, H. E.; Fultz, W. C.; Tam, W. *Organometallics* **1985**, *4*, 939.
(7) Bryndza, H. E. *Organometallics*, **1985**, *4*, 406.

0002-7863/91/1513-6499$02.50/0

Scheme II

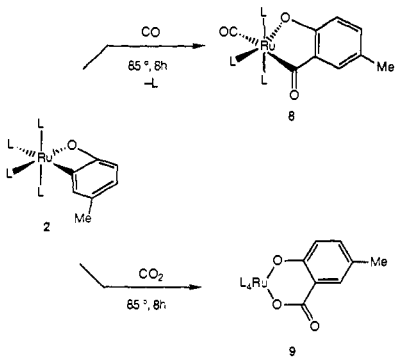

have proposed ionic mechanisms, while others have proposed concerted ones.[5a,c] In our laboratories we observed what may be a model for an intermediate in CO_2 insertion reactions, the direct product of the addition of *tert*-butyl isocyanate to an azairidacylobutane.[8]

In addition to these mechanistic questions, the factors that control selectivity of unsaturated organic compounds toward insertion into the metal–carbon, –nitrogen, and –oxygen bonds are not well understood. The mismatch of a soft late transition metal center and a hard amide or alkoxide substituent has led to the expectation that late metal heteroatom bonds should react preferentially over metal–carbon bonds. This has been the result with some systems,[6a,b,f,g,i] but another system shows preferential M–C over M–O insertion of carbon monoxide.[4b,c] One problem in understanding the migratory aptitudes of these substituents has been the lack of metal–ligand systems in which a series of compounds containing M–C and M–X bonds can be directly and systematically compared.

We report here the reactions of a series of compounds containing ruthenium–carbon, ruthenium–oxygen, and ruthenium–nitrogen bonds to the same L_4Ru (L = PMe_3) fragment. Their insertion reactions with carbon monoxide and carbon dioxide are selective for the metal–carbon bond in some cases and the metal–heteroatom bond in other cases. We have been able to obtain mechanistic data for the insertion reactions of CO_2, including the observation of probable reaction intermediates.

Results

The synthesis of the ortho metalated benzyl compound, $L_4Ru(\eta^2\text{-}CH_2C_6H_4)$ (L = PMe_3) (**1**) (Scheme I), was reported by Wilkinson in 1984.[9] We have described the analogous ortho metalated aryloxide complex $L_4Ru(OC_6H_3Me)$ (**2**) (Scheme II)[10] and have reported the preparation of the ortho metalated arylamide complexes $L_4Ru(NHC_6H_4)$ (**3**) (Scheme III)[11] and $L_4Ru(NHC_6H_3CMe_3)$ (**4**). For the purpose of reference, the ^1H, $^{31}P\{^1H\}$, and $^{13}C\{^1H\}$ NMR spectral data for compounds **1**–**3** are included in Tables I–III. In this paper we describe the insertion reactions of these three compounds with CO and CO_2.

Insertion Reactions of the Ortho Metalated Benzyl Complex $L_4Ru(\eta^2\text{-}CH_2C_6H_4)$. The products of reaction of the known ortho metalated benzyl complex **1** with CO and CO_2 are shown in Scheme I. The reaction of **1** with 2 atm of carbon monoxide in benzene led to formation of **5**, the result of insertion into the metal–aryl bond and substitution of carbon monoxide for a phosphine ligand. Reaction of **1** with 1 equiv of carbon dioxide in benzene led predominantly (90–95%) to formation of **6**, the product of insertion into the metal–aryl bond. Isolation of this product in crystalline form was achieved by cooling a solution of **6** which contained excess trimethylphosphine. It was necessary to conduct solution spectroscopic analysis in the presence of added PMe_3 because in its absence the tris-phosphine complex **7** (see below) is formed. Elemental and mass spectral analysis for **6** were unsatisfactory, presumably due to this instability. However, the structure of **6** could be determined on the basis of ^1H, $^{31}P\{^1H\}$, and $^{13}C\{^1H\}$ NMR spectral analysis in a sealed tube containing 2 equiv of added phosphine.

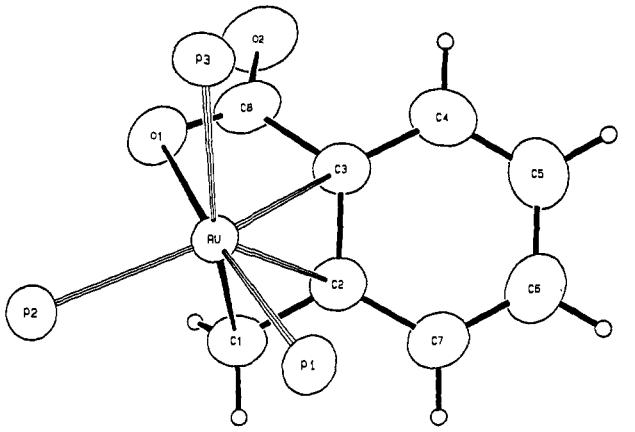

Figure 1. ORTEP drawing of **7**. The methyl groups of the PMe_3 ligand have been omitted for clarity.

Scheme III

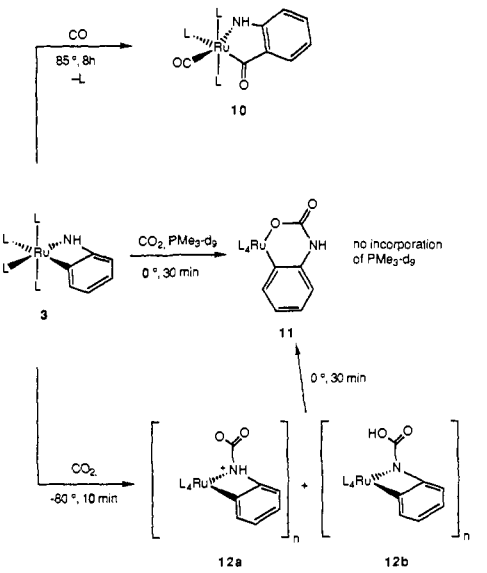

When the addition of CO_2 was conducted for 2 days at 85 °C in *n*-pentane instead of an arene solvent the tris-phosphine complex **7** (observed as the minor product in the reaction of **1** with CO_2 in arene solvent, and observed in all solutions of **6** without added phosphine) crystallized from solution. Although complex **7** displayed fluxional behavior in solution spectroscopic studies, an X-ray diffraction study conducted on a single crystal of **7** is consistent with the NMR data obtained at −10 °C provided in the tables. Evidence for at least two different fluxional processes was obtained by ^1H NMR spectroscopy, but the low- and high-temperature regimes could not be reached for either process. An ORTEP drawing is shown in Figure 1; bond distances and angles for **7** are provided in Tables V and VI.

The presence of phosphine ligands in the ruthenium coordination sphere provided information critical to the determination of which Ru–X bond was involved in the insertion reaction. The splitting patterns for the metal-bound carbon atoms display coupling to all of the coordinated phosphine ligands. This coupling is lost upon insertion of CO or CO_2. For example, The $^{13}C\{^1H\}$ NMR spectrum of the CO insertion product **5** showed a doublet of triplets pattern for the benzylic CH_2 group, due to coupling to one trans and two cis phosphorus nuclei, similar to that observed for starting complex **1**. The large ^{31}P–^{13}C coupling constant (J = 48.8 Hz)

(8) Klein, D. P.; Hayes, J. C.; Bergman, R. G. *J. Am. Chem. Soc.* **1988**, *110*, 3704.
(9) Slatler, J. A.; Wilkinson, G.; Thornton-Pett, M.; Hursthouse, M. B. *J. Chem. Soc., Dalton Trans.* **1984**, 1731.
(10) Hartwig, J. F.; Bergman, R. G.; Andersen, R. A. *J. Organomet. Chem.* **1990**, *394*, 417.
(11) Hartwig, J. F.; Bergman, R. G.; Andersen, R. A. *J. Am. Chem. Soc.* **1991**, *113*, 3404.

Table 1. ^1H NMR Spectroscopic Data[a]

δ, ppm	mult[a]	J, Hz	integral	assign[b]
	$(PMe_3)_4Ru(\eta^2\text{-}CH_2C_6H_4)$ (1)[d]			
0.93	d	5	9	*cis*-PMe_3
1.17	d	5	9	
1.03	t	3	18	*trans*-PMe_3
1.35	m		2	CH_2
6.61	d	7	1	aromatic
7.11	t	7	1	
7.20	t	7	1	
7.52	d	7	1	
	$(PMe_3)_3(CO)Ru(\eta^2\text{-}CH_2C_6H_4C(O))$ (5)[f]			
1.14	t	3.1	18	*trans*-PMe_3
1.49	d	6.7	9	*cis*-PMe_3
2.65	td	7.6, 4.4	2	CH_2
6.84	td	13.8, 0.7	1	aromatic
7.04	td	7.4, 1.3	1	
7.09	d	7.6	1	
7.35	d	7.5	1	
	$(PMe_3)_4Ru(\eta^2\text{-}OC(O)C_6H_4CH_2)$ (6)[d]			
0.81	d	7.4	9	*cis*-PMe_3
1.10	d	5.9	9	
0.97	t	2.7	18	*trans*-PMe_3
2.44	m		2	CH_2
7.15	m		1	aromatic
7.20	t	7.2	1	
7.43	d	7.3	1	
8.84	d	7.6	1	
	$(PMe_3)_3Ru(\eta^4\text{-}OC(O)C_6H_4CH_2)$ (7)[e]			
0.35	d	8.1	9	PMe_3
1.13	d	9.7	9	
1.14	d	6.8	9	
1.69	m		1	CH_2
2.43	m		1	
6.86	t	6.8	1	aromatic
7.00	m		2	
8.43	m		1	
	$(PMe_3)_4Ru(\eta^2\text{-}OC_6H_3Me)$ (2)[f]			
1.00	d	7.4	9	*cis*-PMe_3
1.09	d	6.0	9	
1.15	t	5.8	18	*trans*-PMe_3
2.58	s		3	*p*-Me
6.06	d	7.6	1	aromatic
6.96	d	7.2	1	
7.30	br, s		1	
	$(PMe_3)_3(CO)Ru(\eta^2\text{-}OC_6H_3(Me)C(O))$ (8)[d]			
0.97	t	5.2	18	*trans*-PMe_3
1.17	d	7.7	9	*cis*-PMe_3
2.28	s		3	Me
7.13	d	9.2	1	aromatic
7.27	d	9.3	1	
7.74	br, s		1	
	$(PMe_3)_4Ru$ $(\eta^2\text{-}OC_6H_3(Me)C(O)O)$ (9)[c]			
1.24	t	3.1	18	*trans*-PMe_3
1.37	d	2.14	9	*cis*-PMe_3
1.39	d	2.31	9	
2.11	s		3	Me
6.42	d	8.3	1	aromatic
6.76	dd	8.2, 2.5	1	
7.71	d	2.4	1	
	$(PMe_3)_4Ru(\eta^2\text{-}NHC_6H_4)$ (3)[d]			
0.98	d	5.7	9	*cis*-PMe_3
1.06	d	6.7	9	
1.13	t	2.3	18	*trans*-PMe_3
1.28	br, s		1	NH
5.84	d	7.4	1	aromatic
6.65	t	6.5	1	
7.11	t	7.3	1	
7.33	br, s		1	
	$(PMe_3)_3(CO)Ru(\eta^2\text{-}NHC_6H_4C(O))$ (10)[d]			
0.93	t	3.3	18	*trans*-PMe_3
1.23	d	8.1	9	*cis*-PMe_3
3.12	br, s		1	NH
6.37	m		1	aromatic
6.64	dd	21.4, 8.3	1	
7.07	m		1	
7.81	t	7.6	1	
	$(PMe_3)_4Ru(\eta^2\text{-}OC(O)NHC_6H_4)$ (11)[c]			
0.93	d	6.6	9	*cis*-PMe_3
1.07	d	5.8	9	
0.94	t	2.9	18	*trans*-PMe_3
6.43	d	7.7	1	aromatic
6.76	t	7.0	1	
6.96	t	7.2	1	
7.25	m		1	
7.48	br, s		1	NH
	$(PMe_3)_4Ru(\eta^2\text{-}NHC_6H_4C(O)O)$ (13)[c]			
1.25	t	2.8	18	*trans*-PMe_3
1.33	d	7.6	9	*cis*-PMe_3
1.40	d	7.6	9	
2.35	br, s		1	NH
5.85	t	7	1	aromatic
6.21	d	8	1	
6.65	t	7	1	
7.77	d	8	1	

[a] The symbols d and t, when applied to the PMe_3 resonances, are observed patterns, not true multiplicity patterns. Accordingly, the values reported as coupling constants for these resonances are the separation between lines and do not necessarily reflect the true coupling constants. [b] The assignments of cis and trans for the PMe_3 ligands refers to the mutually cis and mutually trans PMe_3 sites. [c] CD_2Cl_2. [d] C_6D_6. [e] THF-d_8, −10 °C. [f] THF-d_8.

indicated that a phosphine was located trans to the CH_2. Since the other phosphines are located trans to each other (A_2B pattern in the $^{31}P\{^1H\}$ NMR spectrum), the coordinated CO must be located trans to the inserted CO.

The $^{31}P\{^1H\}$ NMR chemical shifts of the phosphine ligands reflect the nature of the substituent which is located trans to it,[12] and this property is also useful in identifying $L_4Ru(X)(Y)$ compounds. Many complexes with the formula *cis*-$(PMe_3)_4Ru(X)(Y)$ (X, Y = alkyl or hydride) have been synthesized,[5d,11,13] and the $^{31}P\{^1H\}$ NMR spectra of these complexes show chemical shifts for the phosphine ligands trans to the alkyl or hydride which are upfield from the chemical shift of the two mutually trans phosphines. When X or Y corresponds to π-donors such as chloride[9,11] or acetate,[14] the chemical shift of the phosphine ligand trans to it is observed downfield from the chemical shift of the mutually trans phosphines. These trends in chemical shift are due to the high trans influence of the alkyl group and the low trans influence of the halide substituent relative to the phosphine ligand.[12] For example, the $^{31}P\{^1H\}$ NMR spectrum of CO_2 insertion product **6** displayed an A_2BC pattern with P_B resonating upfield and P_C resonating downfield from P_A, indicating that a reaction had occurred to form a ruthenium–oxygen bond.

Insertion Reactions of the Ortho Metalated Ruthenium Cresolate Complex $L_4Ru(\eta^2\text{-}OC_6H_3Me)$. The insertion reactions of the ortho metalated cresolate complex **2** are shown in Scheme II. The

(12) A trans influence series is given in: Appleton, T. G.; Clark, H. C.; Manzer, L. E. *Coord. Chem. Rev.* **1973**, *10*, 335. Discussion of correlations between trans influence and ^{31}P chemical shifts is found in: (a) Nixon, G. F.; Pidcock, A. *Annu. Rev. NMR Spectrosc.* **1969**, *2*, 345. (b) Verkade, J. M.; Quin, L. D. Eds. *Phosphorus-31 NMR Spectroscopy in Stereochemical Analysis*; VCH Publishers: New York, 1987. (c) Meek, D. W.; Mazanec, T. J. *Acc. Chem. Res.* **1981**, *14*, 266.

(13) (a) Andersen, R. A.; Jones, R. A.; Wilkinson, G. *J. Chem. Soc., Dalton Trans.* **1978**, *446*. (b) Wong, W-K.; Chiu, K. W.; Statler, J. A.; Wilkinson, G.; Motevalli, M.; Hursthouse, M. B. *Polyhedron* **1984**, *3*, 1255.

(14) Mainz, V. V.; Andersen, R. A. *Organometallics* **1984**, *3*, 675.

Table II. $^{13}C\{^1H\}$ NMR Spectroscopic Data[a]

δ, ppm	mult[a]	J, Hz	assignt[b]	δ, ppm	mult[a]	J, Hz	assignt[b]
	$(PMe_3)_4Ru(\eta^2\text{-}CH_2C_6H_4)$ (1)[d]				$(PMe_3)_4Ru(\eta^2\text{-}OC_6H_3(Me)C(O)O)$ (9)[c]		
−3.5	dq	51, 8	CH_2	17.52	t	12.7	*trans*-PMe_3
19.7	it	13, 4	*trans*-PMe_3	21.09	d	30.3	*cis*-PMe_3
24.5	dm	14	*cis*-PMe_3	21.37	d	27.40	
26.1	dm	12		20.33	s		Me
120.2	s		aromatic	119.59	s		aromatic
122.9	s			121.38	s		
124.1	s			123.84	d	4.6	
138.0	s			132.18	s		
	$(PMe_3)_3(CO)Ru(\eta^2\text{-}CH_2C_6H_4C(O))$ (5)[f]			133.79	s		
18.93	td	15, 3	*trans*-PMe_3	168.86	s		
21.56	d	22.1	*cis*-PMe_3	170.61	s		OC(O)
21.06	dt	48.8, 10.1	CH_2		$(PMe_3)_4Ru(\eta^2\text{-}NHC_6H_4)$ (3)[c]		
117.94	s		aromatic	19.57	tt	12.9, 1.8	*trans*-PMe_3
123.58	s			23.37	dt	16.8, 2.2	*cis*-PMe_3
129.44	s			25.32	dm	20.0	
130.00	d	6.9		105.28	m		aromatic
153.75	d	2.3		111.09	m		
162.04	s			122.78	s		
206.15	m		M–CO	136.38	m		
274.50	m		M–C(O)–Ar	142.97	dtd	64.3, 15.9, 7.5	
	$(PMe_3)_4Ru(\eta^2\text{-}OC(O)C_6H_4CH_2)$ (6)[d]			178.84	d	4.0	
16.08	dq	53.7, 9.2	CH_2		$(PMe_3)_3(CO)Ru(\eta^2\text{-}NHC_6H_4C(O))$ (10)[d]		
19.18	t	12.21	*trans*-PMe_3	17.93	t	14.7	*trans*-PMe_3
21.98	d	17.4	*cis*-PMe_3	20.57	d	27.6	*cis*-PMe_3
23.43	d	26.3		109.20	s		aromatic
122.70	s		aromatic	115.50	d	4.6	
127.69	s			120.94	s		
132.67	s			131.97	s		
132.74	s			134.02	s		
139.64	s			169.11	s		
152.65	s			202.77	m		M–CO
171.08	s		OC(O)	205.39	m		M–C(O)–Ar
	$(PMe_3)_3Ru(\eta^4\text{-}OC(O)C_6H_4CH_2)$ (7)[e]				$(PMe_3)_4Ru(\eta^2\text{-}OC(O)NHC_6H_4)$ (11)[c]		
19.70	d	26.3	PMe_3	19.17	id	13.0, 1.8	*trans*-PMe_3
20.45	d	21.2		21.53	d	18.3	*cis*-PMe_3
21.25	d	37.8		24.48	d	25.8	
37.30	d	25.8	CH_2	113.49	s		aromatic
102.47	d	4.3	aromatic	118.27	s		
118.09	s			122.11	s		
121.05	s			145.95	d	0.9	
130.37	s			148.18	s		
132.14	s			150.27	dm	73.6	
137.29	s			157.57	s		OC(O)
169.54	s		OC(O)		$(PMe_3)_4Ru(\eta^2\text{-}NHC_6H_4C(O)O)$ (13)[c]		
	$(PMe_3)_4Ru(\eta^2\text{-}OC_6H_3Me)$ (2)[f]			18.05	t	12.9	*trans*-PMe_3
18.65	id	13.5, 3.0	*trans*-PMe_3	21.09	d	25.0	*cis*-PMe_3
22.44	di	18.1, 2.6	*cis*-PMe_3	22.00	d	27.4	
25.32	dq	25.0, 3.4		107.63	s		aromatic
21.88	s		*p*-Me	115.43	s		
105.55	s		aromatic	121.08	d	5.1	
120.44	s			129.86	s		
122.00	s			134.72	s		
137.80	s			160.36	s		
142.69	did	65, 16, 6		170.68	s		O(C)O
182.41	s				$(PMe_3)_4Ru(\eta^2\text{-}OC(O)C_6H_3NH_2)$ (17)[c]		
	$(PMe_3)_3(CO)Ru(\eta^2\text{-}OC_6H_3(Me)C(O))$ (8)[d]			18.63	td	13.2, 2.4	*trans*-PMe_3
17.16	i	14.5	*trans*-PMe_3	22.29	dt	20.3, 1.8	*cis*-PMe_3
20.50	d	30.0	*cis*-PMe_3	24.99	did	25.9, 4.0, 1.8	
20.48	s		Me	109.19	s		aromatic
118.53	s		aromatic	124.66	d	2.7	
120.07	s			129.00	dd	3.7, 1.7	
120.32	s			129.64	dd	4.4, 1.6	
133.44	s			148.86	s		
139.34	s			181.76	dtd	70.8, 14.9, 7.9	
177.90	s			183.50	d	10.0	OC(O)
202.68	s		M–CO				
265.38	m		M–C(O)–Ar				

[a] The symbols d and i, when applied to the PMe_3 resonances, are observed patterns, not true multiplicity patterns. Accordingly, the values reported as coupling constants for these resonances are the separation between lines and do not necessarily reflect the true coupling constants. [b] The assignments of cis and trans for the PMe_3 ligands refers to the mutually cis and mutually trans PMe_3 sites. [c] CD_2Cl_2. [d] C_6D_6. [e] THF-d_8, −10 °C. [f] THF-d_8.

reaction of $L_4Ru(\eta^2\text{-}OC_6H_3Me)$ (**2**) with 2 atm of carbon monoxide at 85 °C for 8 h formed compound **8** in 51% isolated yield. This product resulted from insertion of carbon monoxide into the metal carbon bond of **2** and substitution of carbon monoxide for

Table III. $^{31}P\{^1H\}$ NMR Spectroscopic Data

spin system	δ, ppm	J, Hz
	$(PMe_3)_4Ru(\eta^2\text{-}CH_2C_6H_4)$ (**1**)[b]	
A_2BC	$\delta_A = -5.6$	$J_{AB} = 27$
	$\delta_B = -10.4$	$J_{AC} = 27$
	$\delta_C = -10.7$	$J_{BC} = 13$
	$(PMe_3)_3(CO)Ru(\eta^2\text{-}CH_2C_6H_4C(O))$ (**5**)[d]	
A_2B	$\delta_A = -4.01$	$J_{AB} = 27.0$
	$\delta_B = -15.49$	
	$(PMe_3)_4Ru(\eta^2\text{-}OC(O)C_6H_4CH_2)$ (**6**)[b]	
A_2BC	$\delta_A = -1.34$	$J_{AB} = 35.5$
	$\delta_B = 14.12$	$J_{AC} = 24.6$
	$\delta_C = -14.00$	$J_{BC} = 15.1$
	$(PMe_3)_3Ru(\eta^4\text{-}OC(O)C_6H_4CH_2)$ (**7**)[c]	
ABC	$\delta_A = 24.80$	$J_{AB} = 43.4$
	$\delta_B = 17.34$	$J_{AC} = 6.6$
	$\delta_C = -10.81$	$J_{BC} = 28.2$
	$(PMe_3)_4Ru(\eta^4\text{-}OC_6H_3(Me))$ (**2**)[b]	
A_2BC	$\delta_A = -2.73$	$J_{AB} = 34$
	$\delta_B = 15.78$	$J_{AC} = 24$
	$\delta_C = -9.31$	$J_{BC} = 17$
	$(PMe_3)_3(CO)Ru(\eta^2\text{-}OC_6H_3(Me)C(O))$ (**8**)[b]	
A_2B	$\delta_A = -2.57$	$J_{AB} = 30.8$
	$\delta_B = 7.54$	
	$(PMe_3)_4Ru(\eta^2\text{-}OC_6H_3(Me)C(O)O)$ (**9**)[a]	
A_2BC	$\delta_A = 1.14$	$J_{AB} = 17$
	$\delta_B = 11.35$	$J_{AC} = 17$
	$\delta_C = 14.35$	$J_{BC} = 17$
	$(PMe_3)_4Ru(\eta^2\text{-}NHC_6H_4)$ (**3**)[b]	
A_2BC	$\delta_A = -4.01$	$J_{AB} = 32.7$
	$\delta_B = 6.56$	$J_{AC} = 23.9$
	$\delta_C = -10.89$	$J_{BC} = 17.6$
	$(PMe_3)_4Ru(\eta^2\text{-}NHC_6H_4)$ (**3**-^{15}N)[b]	
A_2BCX ($X = {}^{15}N$)	$\delta_A = -4.01$	$J_{AB} = 32.6$
	$\delta_B = 6.42$	$J_{AC} = 24.1$
	$\delta_C = -10.89$	$J_{BC} = 17.6$
		$J_{BX} = 30.7$
	$(PMe_3)_3(CO)Ru(\eta^2\text{-}NHC_6H_4C(O))$ (**10**)[b]	
A_2B	$\delta_A = -1.35$	$J_{AB} = 31.4$
	$\delta_B = -4.79$	
	$(PMe_3)_4Ru(\eta^2\text{-}OC(O)NHC_6H_4)$ (**11**)[b]	
A_2BC	$\delta_A = -2.81$	$J_{AB} = 34.1$
	$\delta_B = 10.39$	$J_{AC} = 24.5$
	$\delta_C = -14.50$	$J_{BC} = 14.9$
	$(PMe_3)_4Ru(\eta^2\text{-}NHC_6H_4C(O)O)$ (**13**)[a]	
A_2BC	$\delta_A = 14.11$	$J_{AB} = 29.1$
	$\delta_B = 1.80$	$J_{AC} = 33.2$
	$\delta_C = 14.11$	$J_{BC} = 28.8$
	$(PMe_3)_4Ru(\eta^2\text{-}OC(O)C_6H_3NH_2)$ (**17**)	
A_2BC	$\delta_A = -2.27$	$J_{AB} = 34.8$
	$\delta_B = 9.23$	$J_{AC} = 25.2$
	$\delta_C = -14.57$	$J_{BC} = 16.1$

[a] CD_2Cl_2. [b] C_6D_6. [c] $C_6H_5Me\text{-}d_8$, −10 °C. [d] THF-d_8.

Table IV. Crystal and Data Parameters for **7**

(A) Crystal Parameters at $T = 25$ °C	
empirical formula, $RuP_3O_2C_{17}H_{33}$	V, 1068.5 (3) Å^3
a, 9.0279 (13) Å	size, 0.20 × 0.20 × 0.20 mm
b, 9.1509 (13) Å	space group, $P\bar{1}$
c, 14.5300 (21) Å	formula wt, 463.4 amu
α, 79.753 (12)°	$Z = 2$
β, 83.175 (12)°	d(calc), 1.44 g cm^{-3}
γ, 64.915 (11)°	μ(calc), 9.5 cm^{-1}

(B) Data Measurement Parameters

radiation, Mo Kα (λ = 0.71073 Å)
monochromator, highly oriented graphite (2θ = 12.2)
detector, crystal scintillation counter, with PHA
reflcns measured, $+h, \pm k, \pm l$
2θ range, 3–45°
scan type, θ–2θ
scan width, $\Delta\theta = 0.55 + 0.35 \tan\theta$
scan speed, 0.66–6.70 (θ, deg/min)
background: meas over 0.25(Δθ) added to each end of the scan
vert aperature, 3.0 mm
horiz aperture, 2.0 + 1.0 tan θ mm
no. of reflcns collected, 2796
no. of unique reflcns, 2796

Table V. Intramolecular Distances (Å) for **7**

atom 1–atom 2	distance	atom 1–atom 2	distance	atom 1–atom 2	distance
Ru–P1	2.262 (1)	C1–C2	1.449 (3)	P1–C9	1.828 (2)
Ru–P2	2.245 (1)	C2–C3	1.436 (2)	P1–C10	1.831 (2)
Ru–P3	2.340 (1)	C2–C7	1.426 (3)	P1–C11	1.813 (2)
Ru–O1	2.170 (1)	C3–C4	1.412 (3)	P2–C12	1.812 (2)
Ru–C1	2.171 (2)	C4–C5	1.356 (3)	P2–C13	1.824 (2)
Ru–C2	2.319 (2)	C5–C6	1.403 (3)	P2–C14	1.829 (2)
Ru–C3	2.411 (2)	C6–C7	1.355 (3)	P3–C15	1.823 (2)
Ru–C8	2.698 (2)	C3–C8	1.500 (3)	P3–C16	1.831 (2)
		C8–O1	1.288 (2)	P3–C17	1.826 (2)
		C8–O2	1.230 (2)		

Table VI. Intramolecular Angles (deg) for **7**

atom 1–atom 2–atom 3	angle	atom 1–atom 2–atom 3	angle
O1–Ru–P1	173.26 (4)	Ru–P1–C9	114.49 (7)
O1–Ru–P2	92.65 (4)	Ru–P1–C10	117.89 (7)
O1–Ru–P3	86.11 (4)	Ru–P1–C11	121.43 (6)
O1–Ru–C1	78.47 (6)	C9–P1–C10	101.55 (10)
C1–Ru–P1	98.85 (5)	C9–P1–C11	100.01 (10)
C1–Ru–P2	92.72 (5)	C10–P1–C11	98.00 (9)
C1–Ru–P3	161.45 (5)	Ru–P2–C12	109.73 (8)
P1–Ru–P2	93.66 (2)	Ru–P2–C13	124.26 (7)
P1–Ru–P3	95.32 (2)	Ru–P2–C14	117.38 (7)
P2–Ru–P3	98.28 (2)	C12–P2–C13	100.58 (10)
Ru–C1–C2	76.81 (10)	C12–P2–C14	101.26 (10)
Ru–O1–C8	99.42 (10)	C13–P2–C14	100.24 (11)
C1–C2–C3	120.74 (16)	Ru–P3–C15	113.00 (8)
C1–C2–C7	122.15 (16)	Ru–P3–C16	115.64 (8)
C3–C2–C7	116.97 (16)	Ru–P3–C17	124.82 (7)
C2–C3–C4	118.14 (17)	C15–P3–C16	100.44 (11)
C2–C3–C8	120.79 (16)	C15–P3–C17	99.72 (12)
C4–C3–C8	119.68 (16)	C16–P3–C17	99.47 (11)
C3–C4–C5	122.60 (18)		
C4–C5–C6	119.64 (19)		
C5–C6–C7	119.88 (18)		
C2–C7–C6	122.65 (17)		
O1–C8–C3	113.63 (15)		
O2–C8–C3	120.10 (20)		
O1–C8–O2	126.23 (19)		

the phosphine ligand trans to the inserted carbon monoxide. There was no evidence for any other products when the reaction was monitored in a sealed NMR tube. The $^{13}C\{^1H\}$ NMR spectrum of the product contained only singlets in the aryl region, indicating that the Ru–C linkage rather than the Ru–O linkage had been broken. The $^{13}C\{^1H\}$ NMR resonance corresponding to the inserted carbon monoxide (δ 265.38) was observed as a multiplet, indicating that this carbon was bound to ruthenium. However, small P–C coupling constants were observed, indicating that the inserted carbon monoxide was bound trans to the coordinated carbon monoxide, rather than to phosphine. The chemical shifts in the $^{31}P\{^1H\}$ spectrum were also consistent with P_B being coordinated trans to the ruthenium–oxygen bond.

Reaction of **2** with 1 equiv of carbon dioxide at 85 °C in a closed vessel led to formation of compound **9**, again resulting from reaction with the metal–carbon bond. Crystals of **9** formed from the reaction solution in 58% yield and were characterized by conventional spectroscopic techniques and combustion analysis. The lack of a multiplet resonance in the aryl region of the $^{13}C\{^1H\}$

NMR spectrum of the product indicated that insertion had occurred into the Ru–C bond. The $^{31}P\{^1H\}$ NMR spectrum indicated that P_B and P_C are coordinated trans to ruthenium–oxygen bonds.

The rate of the insertion reaction showed a marked dependence on phosphine concentration. The reaction of CO_2 (5 equiv) with **2** was conducted in two NMR tubes, side by side, one tube containing no additional phosphine and one tube containing 3 equiv of added phosphine (0.029 M). Monitoring the reactions at 85 °C showed that the half-life for the sample containing no added phosphine was on the order of 45 min, while that for the sample containing 3 equiv of phosphine was roughly 18 h.

Insertion Reactions of the Ortho Metalated Ruthenium Anilide Complex $L_4Ru(\eta^2\text{-}NHC_6H_4)$. Insertion reactions of the ortho metalated anilide complex $(PMe_3)_4Ru(\eta^2\text{-}NHC_6H_4)$ (**3**) are shown in Scheme III. Reaction of **3** with 2 atm of carbon monoxide at 85 °C in benzene led to the formation of compound **10**, the product of insertion into the ruthenium carbon bond, and substitution of CO for the phosphine trans to the metal–nitrogen bond. The product was isolated by crystallization from pentane at −40 °C in 60% yield. Again, the lack of multiplet resonances in the aryl region of the $^{13}C\{^1H\}$ NMR spectrum indicated that insertion had occurred into the metal–aryl bond. The $^{31}P\{^1H\}$ NMR spectrum indicated that P_B was trans to the inserted CO. Therefore, unlike the product of CO with **2**, the best π-acceptor CO is located trans to the better π-donor in **10**, the nitrogen of the ruthenium anilide.[15]

In contrast to reactions of **1** and **2**, the reaction of complex **3** with 1 equiv of carbon dioxide for 20 min at 25 °C yielded **11**, the product of a formal insertion into the metal–nitrogen bond. The white product crystallized from the reaction solution in 57% yield and was characterized by conventional spectroscopic techniques. Compound **11** was insoluble in aromatic hydrocarbon and ether solvents and decomposed in methylene chloride over a period of days, precluding the isolation of crystals suitable for elemental analysis. The $^{13}C\{^1H\}$ NMR spectrum of the product showed an aryl resonance at δ 150.3 with a large $^{31}P\text{–}^{13}C$ coupling constant (J = 73.6 Hz), similar to that observed for the metal-bound aryl resonance in starting material **3** at δ 143.0 ppm. Moreover, the chemical shifts in the $^{31}P\{^1H\}$ NMR spectrum of the product demonstrated that a ruthenium–carbon bond was retained.

When this reaction was monitored at low temperature by NMR spectroscopy, a complex but well-resolved set of spectra was observed which indicated the presence of several reaction intermediates. The reaction of 5 equiv of CO_2 with compound **3** in toluene-d_8 was monitored in the spectrometer probe at 0 °C initially, and two intermediates, attributed to **12a** and **12b**, were observed. The resonances in the $^{31}P\{^1H\}$ NMR spectrum observed after 5 min at 0 °C displayed A_2BC patterns in the $^{31}P\{^1H\}$ NMR spectrum with δ_B resonating downfield and δ_C resonating upfield from δ_A, indicating one ruthenium–oxygen or ruthenium–nitrogen bond and one ruthenium–carbon bond in the structure. Two broad singlets corresponding to OH and NH linkages (vide infra) were observed at 14.3 and 11.9 ppm in the ^1H NMR spectrum under these conditions.

The reaction was monitored by ^1H NMR spectroscopy at 10-deg intervals between 0 and −80 °C. At these temperatures a broad doublet resonance was observed at 1.38 ppm at 0 °C which split into two resonances at −30 °C and separated into five different resonances at −60 °C. In addition, the two resonances observed between 9 and 15 ppm separated into five singlet resonances upon cooling to −80 °C, consistent with at least five intermediates with either NH or OH protons. These five intermediates displayed nearly superimposable $^{31}P\{^1H\}$ NMR spectra, indicating similar connectivity at ruthenium. The $^{13}C\{^1H\}$ NMR spectrum of the reaction of **3** with $^{13}CO_2$ was also consistent with the existence of five intermediates at this temperature. Five $^{13}CO_2$ resonances were observed between 157 and 165 ppm. Upon warming the sample to 30 °C for 0.5 h, all five resonances in the $^{13}C\{^1H\}$ and ^1H NMR spectra disappeared and were replaced by only the signals corresponding to the resonances of product **11**, indicating that this set of five intermediates gives rise to the single product. No reaction was detected between the final insertion product **11** and 5 equiv of CO_2 at room temperature or below.

Information concerning the connectivity of these intermediates was obtained by the use of ^{15}N-labeled starting material. Synthesis of ^{15}N-labeled **3** was performed in the same manner as the synthesis of the unlabeled compound, by the addition of ^{15}N-labeled aniline to the ruthenium benzyne complex $(PMe_3)_4Ru(\eta^2\text{-}C_6H_4)$ (eq 1). The $^{31}P\{^1H\}$ NMR spectrum of the labeled material

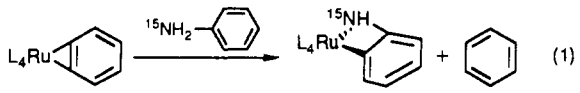

(1)

3-^{15}N

displayed the A_2BC part of an A_2BCX spectrum (X = ^{15}N), with a trans $^{31}P\text{–}^{15}N$ coupling of 30.7 Hz but unresolved cis $^{31}P\text{–}^{15}N$ couplings.

The reaction of **3**-^{15}N with 5 equiv of CO_2 was monitored at −80 °C, following a similar procedure used during the reaction of **3** with CO_2. Again, five intermediates were observed, as demonstrated by the appearance of chemical shifts in the ^1H NMR spectrum indentical with those observed in the reaction of **3** with 5 equiv of CO_2 at −80 °C. However, the pattern of the two farthest upfield resonances in the 9–15-ppm range now appeared as doublets, due to coupling with ^{15}N (J_{NH} = 19 Hz for both),[16] thus assigning these resonances to N–H protons. The three furthest downfield resonances remained singlets in the ^{15}N-labeled case, consistent with assignment as O–H protons. The reaction of **3**-^{15}N with $^{13}CO_2$ was performed under identical conditions, and five resonances in the $^{13}C\{^1H\}$ NMR spectrum were observed at −80 °C, all of which showed coupling to ^{15}N, with J_{CN} ranging from 18 to 19 Hz,[18] confirming the N–CO_2 connectivity.

We do not have a definite structural proposal for all five interconverting reaction intermediates, but based on the spectroscopic data, we propose that they fall into two categories of structures, **12a** and **12b** (Scheme III), which are tautomers. The ^{15}N-labeling experiment clearly demonstrates that all five intermediates contain an N–CO_2 linkage, while three of the intermediates contain OH linkages and two contain NH linkages. The chemical shifts of the $^{31}P\{^1H\}$ NMR spectra of these intermediates indicate that the metal–aryl bond remains intact in all five. Therefore, we are left with the connectivity shown in structures **12a** and **12b**; the existence of rotamers or aggregates of these isomers would explain the observation of more than two intermediates.

To determine qualitatively whether the rate of phosphine dissociation in **3** was competitive with the rate of the insertion reaction, the addition of 10 equiv of CO_2 to **3** was conducted at 0 and 20 °C in the presence of 4 equiv of PMe_3-d_9. Over the course of 2 h at 20 °C, both the reaction to form **11** and the exchange of labeled free phosphine with unlabeled coordinated phosphine occurred.[17] However, at 0 °C, the formation of intermediates **12a** and **12b** as well as their conversion to the final product **11** occurred without any exchange of the free deuterated phosphine with coordinated undeuterated phosphine. Thus, insertion of CO_2 must occur without dissociation of the PMe_3 ligands, consistent with direct attack of CO_2 at the nitrogen atom to form **12a** and **12b**.

We independently synthesized the opposite insertion product in the amide case, i.e. the formal insertion product of CO_2 into the metal–carbon bond, $(PMe_3)_4Ru(\eta^2\text{-}OC(O)C_6H_4NH)$ (**13**) (Scheme IV), with the objective of determining whether the thermodynamic insertion product is **11** or **13** by observing rear-

(15) Collman, J. P.; Hegedus, L. S.; Norton, J. R.; Finke, R. G. *Principles and Applications of Organotransition Metal Chemistry*; University Science Books: Mill Valley, 1987; pp 37 and 58.

(16) For a review of ^{15}N NMR spectroscopy which includes values of $^1H\text{–}^{15}N$, and $^{13}C\text{–}^{15}N$ coupling constants in organic molecules see: Philipsborn, W-n.; Muller, R. *Angew. Chem., Int. Ed. Engl.* **1986**, *25*, 383.

(17) Free PMe_3 and free PMe_3-d_9 can be easily distinguished due to their large isotopic shift in the $^{31}P\{^1H\}$ NMR spectrum.

(18) (a) Hartwig, J. F.; Bergman, R. G.; Andersen, R. A. *Organometallics*, in press. (b) Hartwig, J. F.; Bergman, R. G.; Andersen, R. A. *J. Am. Chem. Soc.* **1990**, *112*, 3234.

(19) Hartwig, J. F.; Andersen, R. A.; Bergman, R. G. Unpublished results.

Scheme IV

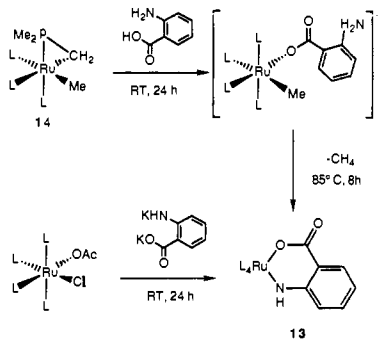

Scheme V

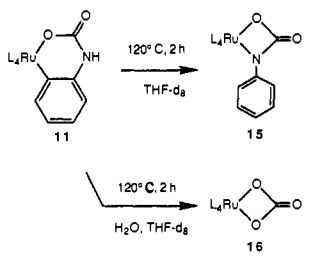

Scheme VI

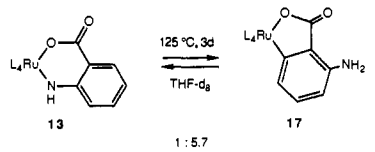

rangement of one to the other. Addition of anthranilic acid (2-aminobenzoic acid) to the previously reported compound $(PMe_3)_4Ru(\eta^2\text{-}CH_2PMe_2)(PMe_3)_3$ (**14**) followed by heating to 85 °C for 8 h led to **13**, which crystallized from the reaction mixture in 73% yield. Alternatively, this complex was prepared in 76% isolated yield by room temperature addition of the dianion of anthranilic acid to the acetate chloride complex $(PMe_3)_4Ru(OAc)(Cl)$ in THF.

Both **11** and **13**, containing six-membered metallacycles, were stable at the conditions under which the conversion of **3** to **11** occurs. Even at higher temperatures, no interconversion of **11** and **13** is observed. Instead both complexes were cleanly converted to products resulting from ring contraction. Heating the direct insertion product **11** to 120 °C for 2 h formed the carboxamide complex $(PMe_3)_4Ru(N(Ph)C(O)O)$ (**15**) as shown in Scheme V. Compound **15** has been independently prepared by the addition of phenyl isocyanate to the oxametallacyclobutane $(PMe_3)_4Ru(OC(Me)(Ph)CH_2)$ during the course of another study and was fully characterized.[18] The carbonate complex $(PMe_3)_4Ru(CO_3)$ (**16**)[19] was the major product when a THF-d_8 solution of **11** was heated under these conditions in the presence of added water.

Rearrangement of **13** required prolonged heating at these temperatures. Thermolysis of THF solutions of **13** at 125 °C for 3 days led to formation of a 5.7 ± 0.6:1 mixture of the O and C bound anthranilate, $(PMe_3)_4Ru(\eta^2\text{-}OC(O)C_6H_3NH_2)$ (**17**), and starting material **13** (96% total yield, ^1H NMR spectroscopy, Cp_2Fe internal standard), as shown in Scheme VI. Neither the direct insertion product **11** nor its thermolysis product, carboxamide **15**, was observed during the course of the reaction. Compound **17** could not be isolated in pure form; roughly the same ratio of **13** and **17** was obtained after crystallization. However, the connectivity of this compound could be determined by ^1H, $^{31}P\{^1H\}$, and $^{13}C\{^1H\}$ NMR spectroscopy, as well as infrared spectroscopy, of the mixture since the data for pure **13** had been obtained. The $^{31}P\{^1H\}$ NMR spectrum displayed an A_2BC pattern, with one resonance upfield and one resonance downfield of the mutually trans phosphine, indicating one Ru–X (X = O or N) and one Ru–C bond. An NH_2 resonance was observed in the ^1H NMR spectrum at δ 5.88 and integrated to twice the intensity of each of the three aryl resonances observed between δ 6.11 and 6.82. Consistent with these data, the $^{13}C\{^1H\}$ NMR spectrum displayed three quaternary resonances and three C–H resonances in the aromatic region, as determined by a DEPT pulse sequence. The infrared spectrum contained a strong absorption at 1584 cm^{-1} corresponding to the carboxylate carbonyl, similar to the frequency of analogous absorptions of **6** and **9**. Two sharp N–H bands were observed at 3384 and 3281 cm^{-1}.

Complete conversion of **13** to **17** was never observed, and it was not straightforward to determine if the 5.7:1 distribution of isomers was an equilibrium ratio. Obtaining samples of **13** and **17** which contained significantly more **17** than the 5.7:1 mixture would have allowed us to clearly demonstrate that this is an equilibrium distribution by observing increasing amounts of **13**. Unfortunately, all samples we obtained by crystallization contained ratios between 3.7:1 and 5.7:1 of **17** to **13**. However, results of kinetic studies on the conversion of **13** to **17** provide evidence that the 5.7:1 mixture is an equilibrium ratio. A first-order plot of the disappearance of **13** showed significant curvature after 2 half-lives for each of several runs, whereas first-order plots for approach to equilibrium showed good linearity. The kinetic experiments were conducted with three concentrations of added phosphine. The rate constants decreased only slightly with increasing phosphine concentration (see Experimental Section for phosphine concentrations and rate constants), and thus our data do not clearly demonstrate the role of added phosphine in this rearrangement. In addition, the crystallized sample of **13** and **17** obtained as a 1:3.7 ratio was heated to 120 °C for 24 h, and ^1H NMR spectroscopy again showed a 1:5.6 ratio of the two compounds, providing convincing evidence that this ratio reflects an equilibrium distribution and that it does not result from decomposition induced by a trace catalyst.

We attempted to synthesize the insertion products opposite to those observed with CO_2 and **1** and **2**. Addition of phenylacetic acid to **14** led to formation of $(PMe_3)_4Ru(Me)(OC(O)CH_2Ph)$ (eq 2). However, this complex remained stable for 2 days at 135

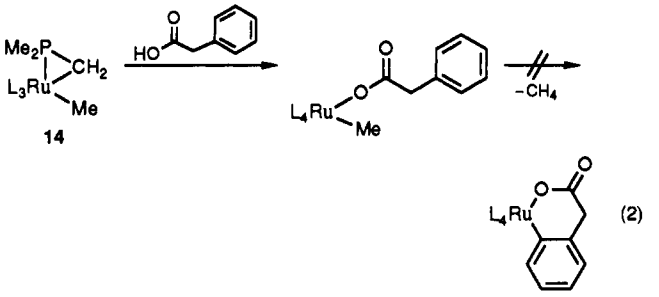

(2)

°C; no formation of methane and the desired ortho metalated product was observed. The addition of $KOC(O)OC_6H_4Me$ to $(PMe_3)_4Ru(Me)Cl$ led to decarboxylation before ortho metalation and formed $(PMe_3)_4Ru(Me)(OC_6H_4Me)$[19] (eq 3).

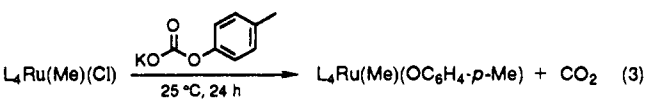

(3)

Discussion

Mechanism. Many mechanistic studies have been conducted concerning the insertion of CO into metal–carbon bonds.[20] These investigations have demonstrated that such reactions normally proceed by initial coordination of the small organic molecule followed by migration of the alkyl or aryl substituent. Our observations on the CO insertion reactions of **1**, **2**, and **3** are consistent with this mechanism. Although these are coordinatively saturated, 18-electron complexes, an open coordination site is readily available by dissociation of phosphine, as demonstrated by the complete exchange of coordinated with uncoordinated phosphine over 2 h at room temperature with compound **3**.

Less mechanistic information is available concerning insertion reactions of CO_2.[21,22] Studies on the reactions of anionic metal

Scheme VII

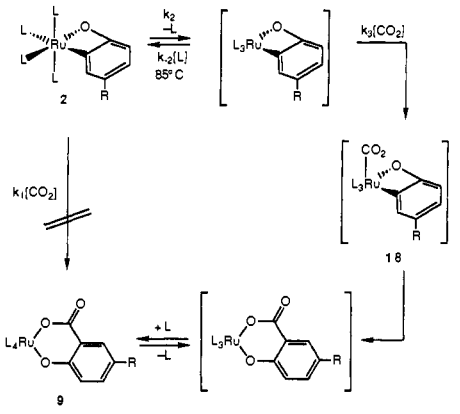

alkyl complexes with CO_2 have shown insertion rates which are faster than that of ligand dissociation, precluding a mechanism involving coordination of the CO_2 and migration of the alkyl group. Yet, mechanistic information on CO_2 deinsertion reactions from formate complexes to form the metal hydride and free CO_2 provide evidence that these processes involve coordinated CO_2 on the reaction pathway.[23]

A coordination and migration mechanism for the insertion of CO_2 into **2** is shown in Scheme VII. The rate expression for a direct insertion mechanism which would not require phosphine dissociation is shown in eq 4. The marked decrease in rate

$$\frac{d[9]}{dt} = k_1[2][CO_2] \tag{4}$$

observed for samples containing added phosphine is inconsistent with this rate law. Rather, it is consistent with eq 5, derived for

$$\frac{d[9]}{dt} = \frac{k_2k_3[2][CO_2]}{k_{-2}[L] + k_3[CO_2]} \tag{5}$$

the mechanism in Scheme VII involving a reversible dissociation of phosphine preceding the rate-determining step of the reaction. This suggests that coordination of CO_2 to form intermediate **18**, followed by migration of the aryl group, leads to the final product.

In contrast to the insertion and deinsertion of CO_2 into the metal–aryl bonds, the reaction of **3** with CO_2 must occur without phosphine dissociation, and low-temperature NMR studies suggest that it is intermediates **12a** and **12b** which are first formed by direct reaction of CO_2 at the nitrogen atom; these species then rearrange to the final product **11**. Thus the formal insertion of CO_2 into the metal–nitrogen bond in the ortho metalated anilide complex **9** proceeds by a pathway different from the coordination/migration mechanism which appears to operate for the metal–carbon bond insertion reactions.

Selectivities. The migratory aptitudes of various alkyl groups toward coordinated CO have been well-studied,[24] and in general benzyl groups undergo migratory insertion reactions slower than aryl groups. Much less studied is a comparison of the relative rates of the migration of alkoxide and amide groups versus those of aryl and alkyl groups. The tetrakis(phosphine)ruthenium system provides a unique spectrum of substituents on the metal

Scheme VIII

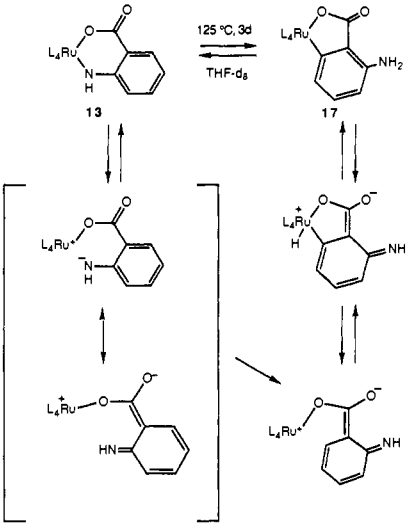

center that can be used to address this question. In addition to the reactions of the four-membered metallacycles reported in this paper, we have recently generated another four-membered metallacycle, an oxaruthenacyclobutane complex. Upon addition of carbon monoxide, this complex undergoes insertion of CO into the metal–carbon bond rather than the metal–oxygen bond.[25] Thus, in all the $(PMe_3)_4Ru(X)(Y)$ compounds that we have examined, the metal–oxygen and metal–nitrogen bonds are remarkably inert toward insertion of carbon monoxide; in all cases, migration of the alkyl or aryl substituent is faster than migration of the heteroatom-containing substituent.

Carbon dioxide shows different reactivity toward aryloxide and amide substituents. CO_2 undergoes overall reaction with the metal–carbon bond in the cyclometalated cresolate **2** and with the metal–nitrogen bond in cyclometalated anilide **3**. We were able to prepare the alternative (M–C) insertion product in the nitrogen case, to establish that M–N insertion is the kinetically determined pathway. Unfortunately, despite several attempts we were not able to independently generate the compound that would have been formed by M–O insertion of CO_2 into **2**, and so the kinetic selectivity must be considered a tentative rather than a rigorous conclusion in this system. If both processes do reflect kinetic selectivities, however, our results are consistent with the reasonable hypothesis that insertion of CO_2 into the metal–carbon bonds proceeds by initial coordination to the metal center, followed by migration of the aryl substituent, and reaction with **3** proceeds by direct attack of the anilide nitrogen atom on CO_2. It appears that the high nucleophilicity of the anilide nitrogen atom relative to the aryloxide oxygen atom accounts for the mechanistic and selectivity differences between these two compounds.

Rearrangements. Several of the six-membered heterometallacycles prepared in this study rearrange thermally to isomers containing smaller ring systems. Compound **6** dissociates phosphine to form the tris-phosphine complex **7**, which crystallizes from the reaction solution when run in alkane solvent. When the reaction was run in arene solvents, the ratio of **6** to **7** was roughly 9:1, implying that the formation of **6** in alkane solvents is driven by the insolubility of **7**.

We believe that the rearrangements of **11** and **13**, each containing 6-membered rings, are driven by the thermodynamic stability of 4- and 5-membered-ring systems in the products. Our qualitative kinetic results suggest that the rearrangement of **13** does not involve initial phosphine loss (we believe the slight inhibition by added PMe_3 is too weak) and is not catalyzed by water. Instead, we propose that the reaction proceeds by a mechanism such as the one shown in Scheme VIII. Dissociation of the arylamide portion of the metallacycle may be driven by delo-

(20) Yamamoto, A. *Organotransition Metal Chemistry*; Wiley: New York, 1986.

(21) Darensbourg, D. J.; Kudaroski, R. A. *Adv. Organomet. Chem.* **1983**, *22*, 129. (b) Behr, A. *Angew. Chem., Int. Ed. Engl.* **1988**, *27*.

(22) (a) Darensbourg, D. J.; Hanckel, R. K.; Bauch, C. G.; Pala, M.; Simmons, D.; White, J. N. *J. Am. Chem. Soc.* **1985**, *107*, 7463. (b) Gröisch, G.; Darensbourg, D. J. *J. Am. Chem. Soc.* **1985**, *107*, 7473.

(23) See for example: (a) Darensbourg, D. J.; Wiegreffe, P.; Riordan, C. G. *J. Am. Chem. Soc.* **1990**, *112*, 5759. (b) Darensbourg, D. J.; Fischer, M. B.; Schmidt, R. E., Jr.; Baldwin, B. *J. Am. Chem. Soc.* **1981**, *103*, 1297. (c) Merrifield, J. H.; Gladysz, J. A. *Organometallics* **1983**, *2*, 782.

(24) Alexander, J. J. *The Chemistry of the Metal–Carbon Bond*; Hartley, F. R., Ed.; Wiley: New York, 1985; Vol. 2, Chapter 5.

(25) Hartwig, J. F.; Bergman, R. G.; Andersen, R. A. *J. Am. Chem. Soc.* **1990**, *112*, 3234.

calization of the resulting negative charge, through the aromatic ring, into the carbonyl group adjacent to the nitrogen atom (see resonance structures in Scheme VIII). Rotation of the resulting η^1-bound organic ligand allows the proper geometry for addition of the aromatic C–H bond, and proton transfer leads to the final rearrangement product **17**. Because it appears that compounds **13** and **17** are in equilibrium, each step in Scheme VIII must be reversible. We have no information at present about whether proton transfer between the metal center and the uncoordinated nitrogen atom occurs in an inter- or intramolecular manner. It seems likely that trace acid catalysts may facilitate these steps, although water does not appear to be acidic enough to affect the reaction rates.[26]

The conversion of **11** to **15** may also involve proton-transfer processes. Although protonolysis of the metal–aryl bond by the amide N–H would form **15**, proton transfer by an acid catalyst formed under the 120 °C reaction conditions may assist this transformation.

Experimental Section

General. Unless otherwise noted, all manipulations were carried out under an inert atmosphere in a Vacuum Atmosphere 553-2 drybox with attached M6-40-1H Dritrain, or by using standard Schlenk or vacuum line techniques as described in previous papers.[10,11]

Unless otherwise specified, all reagents were purchased from commercial suppliers and used without further purification. PMe_3 (Strem) was dried over NaK or a Na mirror and vacuum transferred prior to use. CO and CO_2 (bone dry) were purchased from Matheson. Anthranilic acid was dried by azeotroping with benzene with use of a Dean-Stark trap and then purified by sublimation.

Pentane and hexane (UV grade, alkene free) were distilled from $LiAlH_4$ under nitrogen. Benzene and toluene were distilled from sodium benzophenone ketyl under nitrogen. Dichloromethane was either distilled under N_2 or vacuum transferred from CaH_2. Deuterated solvents for use in NMR experiments were dried as their protiated analogues but were vacuum transferred from the drying agent.

$Ru(PMe_3)_3(CO)(\eta^2\text{-}CH_2C_6H_4C(O))$ (5). To a glass reaction vessel fused to a Kontes vacuum adaptor was added 82.8 mg (0.167 mmol) of $Ru(PMe_3)_4(\eta^2\text{-}CH_2C_6H_4)$ (**1**)[9] in 12 mL of toluene. The vessel was degassed by 2 or 3 freeze–pump–thawing cycles and 450 Torr of CO was added with the vessel submerged in liquid nitrogen. This procedure results in addition of ~2 atm of CO at 25 °C. The vessel was heated to 85 °C for 20 min, over which time the solution turned from clear to yellow. The toluene was removed and the residue was crystallized from pentane at −40 °C to yield 59.4 mg (75%) of product. IR 2982 (m), 2969 (m), 2907 (m), 1910 (s), 1594 (m), 1556 (s), 1528 (m), 942 (s); MS (EI) 476 (M^+), 448 ($M - CO^+$). Anal. Calcd for $C_{18}H_{33}O_2P_3Ru$: C, 45.47; H, 7.00. Found: C, 45.62; H, 7.06.

$Ru(PMe_3)_4(\eta^2\text{-}OC(O)C_6H_4CH_2)$ (6). Into a glass reaction vessel fused to a Kontes vacuum adaptor was placed 250 mg (0.505 mmol) of $Ru(PMe_3)_4(\eta^2\text{-}CH_2C_6H_4)$ (**1**)[9] in 20 mL of benzene. The vessel was degassed by 2 or 3 freeze–pump–thawing cycles, and CO_2 (1.5 equiv, 0.25 mmol) was added by vacuum transfer. The vessel was heated to 85 °C for 16 h. After this time the benzene was removed under reduced pressure. Toluene (~2 mL) and PMe_3 (0.2 mL) were added and the vessel was heated to 85 °C to dissolve the compound and convert any **7** present to **6**. Upon cooling to −40 °C for 12 h, and then −80 °C for 24 h, white crystals of **6** formed. These crystals were collected to yield 128 mg (47%) of product. When the crystals were dissolved in toluene, the solution rapidly turned yellow, indicating some conversion of **6** to **7** had occurred. All solution spectra of **6** were therefore taken in the presence of 2 equiv of PMe_3. Due to the lability of the phosphine ligand, satisfactory mass spectral and microanalytical analyses were not obtained. IR (KBr) 2970 (m), 2910 (m), 1599 (s), 1582 (s), 1551 (s), 1425 (m), 1358 (m), 1300 (m), 1279 (m), 942 (s).

$Ru(PMe_3)_3(\eta^4\text{-}OC(O)C_6H_4CH_2)$ (7). To a glass reaction vessel fused to a Kontes vacuum adaptor was added 88.0 mg (0.178 mmol) of $Ru(PMe_3)_4(\eta^2\text{-}CH_2C_6H_4)$ (**1**)[9] in 7 mL of pentane. The vessel was degassed by 2 or 3 freeze–pump–thawing cycles, and CO_2 (1.5 equiv, 0.267 mmol) was added by vacuum transfer. The vessel was heated to 85 °C for 3 days. The clear solution turned yellow, and over the course of 3 days, yellow crystals formed. The crystals were collected to yield 79.0 mg (96%) of analytically pure **7**. IR (KBr) 2965 (m), 2907 (m), 2851 (m), 1625 (s), 1604 (m), 1428 (m), 1299 (m), 1279 (m), 967 (m), 941 (s); MS (FAB, sulfolane) 465 ($MH1+$), 389 ($MH - PMe_3^+$). Anal. Calcd for $C_{17}H_{33}O_2P_3Ru$: C, 44.06; H, 7.18. Found: C, 44.22; H, 7.27.

$Ru(PMe_3)_3(CO)(\eta^2\text{-}OC_6H_3(Me)C(O))$ (8). To a glass reaction vessel fused to a Kontes vacuum adaptor was added 100 mg (0.196 mmol) of $Ru(PMe_3)_4(\eta^2\text{-}OC_6H_3(Me))$ (**2**)[10] in 20 mL of toluene. The vessel was degassed by freeze–pump–thawing through either 2 or 3 cycles and 450 Torr of CO was added with the vessel submerged in liquid nitrogen. This procedure results in addition of ~2 atm of CO at 25 °C. The vessel was then heated to 85 °C for 8 h, over which time the solution turned darker yellow. The toluene was removed and the residue was crystallized from a toluene–pentane (1:1) solution at −40 °C to yield 54.1 mg (51%) of product. IR 2968 (m), 2911 (m), 1947 (s), 1605 (s), 1551 (s), 1475 (s), 1284 (s), 947 (s); MS (EI) 492 (M^+), 464 ($M - CO^+$), 436 ($M - 2CO^+$). Anal. Calcd for $C_{18}H_{33}O_3P_3Ru$: C, 43.99; H, 6.77. Found: C, 43.80; H, 6.75.

$Ru(PMe_3)_4(\eta^2\text{-}OC_6H_3(Me)C(O)O)$ (9). To a glass reaction vessel fused to a Kontes vacuum adaptor was added a suspension of 100 mg (0.196 mmol) of $Ru(PMe_3)_4(\eta^2\text{-}OC_6H_3(Me))$ (**2**)[10] in 5 mL of toluene. The vessel was degassed by freeze–pump–thawing through either 2 or 3 cycles, and CO_2 (1.5 equiv, 0.29 mmol) was added by vacuum transfer. The vessel was then heated to 85 °C for 8 h over which time period the solution turned clear. Upon cooling, white analytically pure crystals formed and these crystals were collected to yield 62.5 mg (57%) of product. IR 2972 (m), 2911 (m), 1614 (s), 1567 (s), 1479 (s), 1410 (s), 1329 (s), 944 (s); MS (FAB, *p*-nitrobenzyl alcohol) 557 (MH^+), 481 ($MH - PMe_3^+$). Anal. Calcd for $C_{20}H_{42}O_3P_4Ru$: C, 43.24; H, 4.62. Found: C, 42.92; H, 7.41

Reaction of 3 with CO_2 in the Presence of Added Phosphine. In a small vial was weighed 10.0 mg (0.0196 mmol) of **3**, which was then dissolved in 1.2 mL of C_6D_6. An equal amount of the solution was added to two NMR tubes. One of these tubes was degassed by 3 freeze–pump–thaw cycles, 5 equiv (0.0489 mmol) of CO_2 was added by vacuum transfer, and the tube was sealed. The other tube was degassed, and 5 equiv of CO_2 was added followed by 3 equiv (0.0294 mmol) of PMe_3 to give a concentration of 0.049 M. The samples were heated at 85 °C and monitored by ^1H NMR spectroscopy at 0.5, 2, and 18 h. The half life for the reaction with no added phosphine was roughly 0.5 h, while that for the sample containing added phosphine was on the order of 18 h.

$Ru(PMe_3)_3(CO)(\eta^2\text{-}NHC_6H_3(Me)C(O))$ (10). To a glass reaction vessel fused to a Kontes vacuum adaptor was added 80.6 mg (0.163 mmol) of $Ru(PMe_3)_4(\eta^2\text{-}NHC_6H_4)$ (**3**)[11] in 5 mL of toluene. The vessel was degassed by freeze–pump–thawing, and CO (2 atm) was added by exposing the vessel, submerged in liquid nitrogen, to 450 Torr of CO. The vessel was then heated to 85 °C for 16 h, over which time the initial yellow solution turned orange. The solvent was removed under reduced pressure, and the residue was crystallized from a pentane–toluene (10:1) solvent mixture at −40 °C to yield 46.2 mg (60%) of orange crystals. IR (KBr) 3323 (m), 1922 (s), 1599 (s), 1582 (s), 1538 (s), 1479 (s), 1463 (s); MS (EI) 477 (M^+), 449 ($M - CO^+$), 421 ($M - 2CO^+$). Anal. Calcd for $C_{17}H_{32}NO_2P_3Ru$: C, 42.85; H, 6.77; N, 2.94. Found: C, 42.56; H, 6.72; N, 2.96.

$Ru(PMe_3)_4(\eta^2\text{-}OC(O)NHC_6H_4)$ (11). Into a glass reaction vessel fused to a Kontes vacuum adaptor was added 82.0 mg (0.165 mmol) of $Ru(PMe_3)_4(\eta^2\text{-}NHC_6H_4)$ (**3**)[11] in a minimum amount of toluene (~3 mL). The vessel was degassed by freeze–pump–thawing, and CO_2 (1.5 equiv 0.25 mmol) was added by vacuum transfer. The yellow solution rapidly turned clear, and over the course of 4 h clear needles of **11** formed. The vessel was then cooled to −40 °C for 12 h to yield 50.5 mg (56.6%) of product. IR (KBr) 3293 (m), 3187 (m), 2972 (m), 2910 (m), 1639 (s), 1575 (m), 1559 (m), 1490 (m), 1407 (m), 1368 (s), 1300 (m), 1279 (m), 944 (s).

$Ru(PMe_3)_4(\eta^2\text{-}^{15}NHC_6H_4)$ (3-^{15}N). Into a vial was placed 82.6 mg (0.172 mmol) of **1**, 17.1 mg (1.1 equiv) of aniline-^{15}N, and 2 mL of benzene. The solution was then placed in a 9-in. NMR tube which was degassed and sealed. The sample was heated to 110 °C for 8 h. Upon cooling, 58.2 mg (68%) of 3-^{15}N had crystallized from the reaction solution and all of the starting material had been consumed as determined by $^{31}P\{^1H\}$ NMR spectroscopy. The material which had crystallized from solution was pure by ^1H NMR spectroscopy. IR (KBr) 3329 (w), 2968 (m), 2907 (m), 1591 (m), 1559 (m), 1433 (s), 1303 (m), 1282 (s), 943 (s).

Variable-Temperature Study on the Reaction of 3 and 3-^{15}N with CO_2. The ruthenium complex $Ru(PMe_3)_4(\eta^2\text{-}NHC_6H_4)$ (**3**)[11] or $Ru(PMe_3)_4(\eta^2\text{-}^{15}NHC_6H_4)$ (3-^{15}N) (15.5 mg, 0.0313 mmol) was dissolved in 0.7 mL of toluene-d_8 and transferred to a 9 in. medium-walled NMR tube. The sample was freeze–pump–thawed through two cycles and 5 equiv (0.156

(26) A referee has suggested an interesting alternative mechanism: loss of PMe_3 followed by cyclometalation of a coordinated phosphine ligand to give a Ru(IV) intermediate (because of the weak phosphine inhibition result, cyclometalation would have to be substantially more rapid than L recoordination), followed by reductive elimination of an N–H bond, rotation, aryl C–H activation, reductive elimination of the metalated phosphine, and recoordination of PMe_3. Our observations do not rule out this possibility.

mmol) of CO_2 was added by vacuum transfer. The tube was sealed to give a final length of 8 in. The sample was thawed at −78 °C and was placed in the NMR probe, which had been precooled to at least −30 °C. After acquiring the data for the temperature range 0 to −80 °C, the sample was warmed to 30–35 °C and the conversion of **12a** and **12b** to product **11** was observed over the course of 0.5 h.

Thermolysis of 11. A sample of **11** (2.4 mg, 0.0044 mmol), prepared as described above, was dissolved in tetrahydrofuran-d_8 in an NMR tube equipped with a vacuum adaptor, and 1 mg of mesitylene was added as an internal standard. The sample was degassed, sealed, and heated to 120 °C for 2 h. ^1H and $^{31}P\{^1H\}$ NMR spectrometry showed that **15** was the only product formed.

$(PMe_3)_4Ru(\eta^2\text{-}NHC_6H_4C(O)O)$ (13). (a) Addition of anthranilic acid to $(PMe_3)_2Ru(\eta^2\text{-}CH_2PMe_2)(Me)$ (**14**) was accomplished as follows. To a small vial was added 78.2 mg of $(PMe_3)_2Ru(\eta^2\text{-}CH_2PMe_2)(Me)$ (**14**) and 2 mL of benzene. To this solution was added 38.4 mg (1.5 equiv) of anthranilic acid (2-aminobenzoic acid) as a solid. The suspension was stirred for 2 h, after which time ^1H NMR spectroscopy showed that a metal-bound methyl group remained. The solution was then placed into a 9-in. NMR tube, which was equipped with a vacuum adaptor, degassed, and sealed. The sample was heated to 65 °C for 3 h, over which time 74.6 mg (74%) of orange/yellow crystals precipitated from the reaction solution. A portion of the recovered material was recrystallized by vapor diffusion of ether into a tetrahydrofuran solution of **13**. IR (KBr) 3364 (w), 2992 (m), 2972 (m), 2910 (m), 1599 (s), 1560 (s), 1521 (m), 1519 (m), 1473 (s), 1453 (s), 1365 (m), 1355 (m), 1262 (s), 941 (s), 731 (m), 717 (m), 700 (m), 666 (m). Anal. Calcd for $C_{19}H_{41}NOP_4Ru$: C, 42.22; H, 7.65; N, 2.59. Found: C, 42.27; H, 7.73; N, 2.50.

(b) To a solution of 356 mg (0.713 mmol) of $(PMe_3)_4Ru(OAc)(Cl)$ in 10 mL of tetrahydrofuran was added 232 mg (1.5 equiv) of the potassium salt of the dianion of anthranilic acid, $K_2OC(O)C_6H_4NH$, prepared by addition of KH to anthranilic acid in tetrahydrofuran and isolated by filtration. The solution was stirred for 24 h. After roughly 0.5 h the initial pale yellow slurry turned a darker orange/yellow and after an additional 0.5 h it turned back to a paler yellow. Both the anthranilic acid salt and the ruthenium anthranilate product are only sparingly soluble in THF. The tetrahydrofuran solvent was removed under reduced pressure, and the residue was extracted with CH_2Cl_2 and filtered through a plug of Celite. Removal of CH_2Cl_2 under reduced pressure provided 292 mg (76%) of product which was pure enough (~95%) for preparation of the thermolysis product **17**.

$(PMe_3)_4Ru(\eta^2\text{-}OC(O)C_6H_3NH_2)$ (17). (a) Preparative Scale: Into a glass reaction vessel equipped with a Kontes vacuum adaptor was placed a suspension of 252 mg (0.467 mmol) of anthranilate **13** in 15 mL of tetrahydrofuran. The vessel was frozen in liquid nitrogen and exposed to vacuum before the thermolysis at 135 °C for 16 h. At this temperature, the solution is initially yellow and homogeneous. The product is also yellow, but it is very soluble in THF. The solution volume was reduced to 1 mL in vacuo, layered with ether, and cooled to −40 °C to provide 64.6 mg (26%) of a mixture of **13** and **17** as yellow crystals. ^1H, $^{31}P\{^1H\}$, and $^{13}C\{^1H\}$ NMR spectroscopy of this recovered material showed only O- and N-bound anthranilate starting material and the O- and C-bound product in a 1:3.7 ratio. Thermolysis of 2.1 mg of this crystallized material in 0.6 mL of THF-d_8 at 125 °C for 24 h provided a 5.6:1 ratio of **17** to **13**. IR (KBr) 3384 (m), 3281 (w), 2971 (m), 2906 (s), 1584 (s), 1556 (s), 1523 (s), 1430 (m), 1344 (m), 1299 (m), 1279 (m), 970 (m), 942 (s).

(b) Thermolysis with Internal Standard: Into an NMR tube was placed 0.7 mL of a THF-d_8 solution of 10.6 mg (0.0196 mmol) of **13** and 4 mg of ferrocene as an internal standard. The tube was degassed and sealed. An ^1H NMR spectrum was obtained before thermolysis. The NMR tube was submerged in an oil bath heated to 115 °C, and NMR spectra taken periodically over the course of 3 days showed that **13** was converted to a 5.7 ± 6.0:1 ratio of **11**:**13** in 96% overall yield.

Approach to Equilibrium Kinetics for 13 and 17. Into a 5.00-mL volumetric flask was weighed 18.5 mg (0.0343 mmol) of anthranilate **13** and 4.5 mg of mesitylene as internal standard. Tetrahydrofuran-d_8 was added to the flask to make 5.00 mL of solution, with a concentration of 7.5 mM mesitylene. A stirbar was added and the solution was stirred for 8 h. Not all of **13** dissolved, so a typical experiment involved addition of 0.700 mL of the supernatant of this solution by syringe to a thin-walled, 9 in. NMR tube to provide homogeneous samples of **13** and mesitylene. The tube was degassed, PMe_3 was added by vacuum transfer to provide 0.026, 0.099, and 0.143 M solutions, and the tube was flame sealed to give a length of 8.5 in. The concentration of **13** and added phosphine was determined by integrating versus the known concentration of mesitylene internal standard. The tubes were heated at 125 °C in a factory-calibrated Neslab Exocal Model 251 constant temperature bath filled with Dow Corning 200 silicon Fluid. All reactions were monitored by ambient-temperature ^1H NMR spectrometry by integrating mutually trans PMe_3 resonance of the starting material versus that of the mesitylene internal standard. The spectra were taken with a single acquisition and double checked with a second acquisition after a delay of at least 10 T_1. All first-order kinetic plots displayed excellent linearity over the first 2 half-lives with correlation coefficients of 0.99 or better. However, after 2 to 2.5 half-lives the first-order plot deviated from linearity, and the reaction stopped in all three cases at 85% converstion. However, when the data were plotted as a first-order approach to equilibrium (using the 5.7:1 ratio as the infinity point) good linearity ($r^2 \geq 0.98$) was observed for each run. The rates obtained for the three concentrations of phosphine ($2.7 \pm 0.3 \times 10^{-5}$ for 0.026 M, $1.1 \pm 0.1 \times 10^{-5}$ for 0.099 M, and $1.2 \pm 0.1 \times 10^{-15}$ for 0.143 M) did not indicate a strong dependence of reaction rate on phosphine concentration.

Acknowledgment. We are grateful for support of this work from the National Institutes of Health (Grant No. GM-25459). The crystal structure analysis was performed by Dr. F. J. Hollander, staff crystallographer at the UC Berkeley X-ray crystallographic facility (CHEXRAY).

Supplementary Material Available: Tables of positional parameters, anisotropic thermal parametrs, root-mean-square amplitudes of anisotropic displacement, torsion angles, and least-squares plane data for complex **7** (7 pages). These data are provided in the archival edition of the journal, available in many libraries. Alternatively, ordering information is given on any current masthead page.